

Alternative ventilation system for operating theaters: parameter study and full-scale assessment of the performance of a local ventilation system

Loomans, M.G.L.C.; de Visser, I.M.; Loogman, J.G.H.; Kort, H.S.M.

Published in:
Building and Environment

DOI:
[10.1016/j.buildenv.2016.03.012](https://doi.org/10.1016/j.buildenv.2016.03.012)

Published: 22/03/2016

Document Version
Publisher's PDF, also known as Version of Record (includes final page, issue and volume numbers)

Please check the document version of this publication:

- A submitted manuscript is the author's version of the article upon submission and before peer-review. There can be important differences between the submitted version and the official published version of record. People interested in the research are advised to contact the author for the final version of the publication, or visit the DOI to the publisher's website.
- The final author version and the galley proof are versions of the publication after peer review.
- The final published version features the final layout of the paper including the volume, issue and page numbers.

[Link to publication](#)

Citation for published version (APA):

Loomans, M. G. L. C., de Visser, I. M., Loogman, J. G. H., & Kort, H. S. M. (2016). Alternative ventilation system for operating theaters: parameter study and full-scale assessment of the performance of a local ventilation system. *Building and Environment*, 102, 26-38. DOI: 10.1016/j.buildenv.2016.03.012

General rights

Copyright and moral rights for the publications made accessible in the public portal are retained by the authors and/or other copyright owners and it is a condition of accessing publications that users recognise and abide by the legal requirements associated with these rights.

- Users may download and print one copy of any publication from the public portal for the purpose of private study or research.
- You may not further distribute the material or use it for any profit-making activity or commercial gain
- You may freely distribute the URL identifying the publication in the public portal ?

Take down policy

If you believe that this document breaches copyright please contact us providing details, and we will remove access to the work immediately and investigate your claim.



Alternative ventilation system for operating theaters: Parameter study and full-scale assessment of the performance of a local ventilation system



M.G.L.C. Loomans*, I.M. de Visser, J.G.H. Loogman, H.S.M. Kort

Department of the Built Environment, Eindhoven University of Technology, PO Box 513, 5600 MB, Eindhoven, The Netherlands

ARTICLE INFO

Article history:

Received 4 December 2015

Received in revised form

3 March 2016

Accepted 12 March 2016

Available online 16 March 2016

Keywords:

Particle concentration

Air flow analysis

Ventilation efficiency

Air quality

CFD

ABSTRACT

A local operating theater ventilation device to specifically ventilate the wound area has been developed and investigated. The ventilation device is combined with a blanket which lies over the patient during the operation. Two configurations were studied: Configuration 1 where HEPA-filtered air was supplied around and parallel to the wound area and Configuration 2 where HEPA-filtered air was supplied from the top surface of the blanket, perpendicular to the wound area. A similar approach is investigated in parallel for an instrument table. The objective of the study was to verify the effectiveness of the local device. Prototype solutions developed were studied experimentally (laboratory) and numerically (CFD) in a simplified setup, followed by experimental assessment in a full scale mock-up. Isothermal as well as non-isothermal conditions were analyzed. Particle concentrations obtained in proposed solutions were compared to the concentration without local ventilation. The analysis procedure followed current national guidelines for the assessment of operating theater ventilation systems, which focus on small particles ($<10\ \mu\text{m}$). The results show that the local system can provide better air quality conditions near the wound area compared to a theoretical mixing situation (proof-of-principle). It cannot yet replace the standard unidirectional downflow systems as found for ultraclean operating theater conditions. It does, however, show potential for application in temporary and emergency operating theaters.

© 2016 Elsevier Ltd. All rights reserved.

1. Introduction

Between 2002 and 2011, surgical site infections (SSIs) occurred in 2.9% of all surgical operations in conventionally ventilated operating theaters in The Netherlands [1]. SSIs can result in additional surgeries, permanent injuries, or even mortality. In addition to health risks for the patient, SSIs also drive up healthcare costs. Knobben et al. [2] estimated the direct medical costs of treatment of a septic joint, caused by a SSI, at approximately €40,000.

Lidwell et al. [3] found evidence that ultra-clean ventilation in operating theaters (OT) reduces the incidence of SSIs. As a result, the effectiveness of OT ventilation, more specifically horizontal and vertical unidirectional flow (UDF) ventilation systems, has been studied extensively [4–8]. In an 'at rest' situation these systems can achieve a level of ultra-clean air (defined as <10 Colony Forming

Units/ m^3 [CFU/ m^3]; [9]). However, the position of the surgical light and space availability for the operating team and instrument tables can negatively affect performance of this type of ventilation system [10,11]. In addition, in-use assessment of the system in transient conditions has found only limited attention (e.g. Brohus et al. [12]). Furthermore, thermal comfort conditions for the operating personnel can be compromised based on the chosen system solution [13].

In 2014, a new performance based guideline was introduced in The Netherlands [14]. Previous guidelines available generally prescribed design-based solutions, namely the application of vertical UDF systems for high risk surgery. This new guideline offers the opportunity to develop and apply alternative ventilation systems for the operating theater. Performance based requirements in this case are set to the air quality near the operating wound. A prescribed in-situ assessment procedure is available for that. Despite the former design-based requirements, the design and development of alternative operating theater ventilation systems does have a long tradition. Charnley developed a glass-walled chamber, ventilated with filtered clean air [15]. This was further developed

* Corresponding author. Department of the Built Environment, Eindhoven University of Technology, P.O.Box 513, 5600 MB, Eindhoven, The Netherlands.

E-mail address: M.G.L.C.Loomans@tue.nl (M.G.L.C. Loomans).

and investigated by Meierhans and Weber [16]. Babb et al. [17] investigated the application of multiple cabins in one large OT. Whyte et al. [18] compared a conventional mixed ventilation system with a horizontal and vertical UDF system. Local ventilation systems have been developed as well. Levenson et al. [15] describes several designs of isolators and their performance. Specialized solutions have also been proposed for specific types of surgeries like ophthalmic surgery [19] and minimally invasive/laparoscopic surgery [20]. Several researchers also developed and investigated the effectiveness of (mobile) local ventilation systems (e.g. Refs. [21–29]). Klems et al. [30] studied the application of a ring around the wound area, supplying sterile air in combination with a mixed ventilation system. Wound ventilation provides another example of ventilation concepts developed, where CO₂ is used to ventilate the wound [31]. For application in other types of rooms, several examples of personal ventilation concepts have been developed to improve the ventilation efficiency [32–34].

To align with the current potential to introduce innovative operating ventilation systems in the Netherlands and to take into account the work process, the performance of a local ventilation device that ventilates only the wound area was studied. This new device was developed from analysis of key performance indicators for such type of ventilation systems and from earlier examples of innovative ventilation systems discussed above [35]. In the final design, the ventilation device is combined with a surgical blanket covering the patient during the procedure. The idea is to arrive at disposable type of devices.

Two potential configurations have been developed: *Configuration 1*, where HEPA-filtered air was supplied around and parallel to the wound area; and *Configuration 2*, where HEPA-filtered air was supplied from the top surface of the blanket, perpendicular to the wound area. A similar design solution, assuming the same ventilation principle also has been developed for the instrument table. Configuration 1 has some resemblance to the design from Klems et al. [30].

Given the design solution and configurations proposed, the objective of the study was to investigate the effectiveness of these systems in providing a clean area near the wound, to inhibit SSI risk compared to mixing ventilation, while mimicking an in-use situation. Inclusion of the instrument table adds to the total solution.

2. Methods

Fig. 1 and Fig. 2 visualize the two configurations as developed for the local ventilation of the wound area and the instrument table. Analysis of the ventilation performance of the two configurations developed has been conducted in two coordinated steps: 1. *Simplified representation*; 2. *Full-scale mock-up test*. A simplified representation of the ventilation design principle has been developed and tested in a laboratory setting. In these tests sensitivity to design parameters such as supply velocity, turbulence intensity and supply temperature of the HEPA-filtered airflow, and the effect of disturbance by a contaminated airflow over the wound was investigated. Experimental analysis was supported by numerical (CFD) analysis of the same prototype. In the simplified representation, no distinction was made between the ventilated blanket and the instrument table, as focus was on the ventilation principle. In the full-scale mock-up test more realistic prototypes of the configurations, ventilated blanket as well as instrument table, were tested. This test applied a full-scale mockup of an OT to indicate the proof-of-concept. The full-scale tests were only performed experimentally. The remainder of the paper will first explain the methods that have been developed and applied for the two steps. Next the results and discussion of these results will be presented for the two steps separately. An overall discussion and final conclusions will complete the paper.

2.1. Simplified representation

A parameter study was performed on a simplified model of the configurations (box: 1.00 m × 1.00 m × 1.11 m (L × W × H)) that still included the general principles of the functioning of the device. The simplified model encompasses patient's wound area (0.4 m × 0.4 m × 0.11 m) and its immediate surrounding (Fig. 3). It includes a unidirectional sideways contaminated airflow with constant velocity (V_{cont}). This flow combines the disturbance from the operating team, as can be expected in an operating procedure, with the important contaminant source in an OT that they represent as well [37]. The exhaust is positioned on the opposite side. The top and remaining vertical panes are closed. Clean HEPA-filtered (H14 filter class) air was supplied with a constant velocity (V_{HEPA}) around the wound in both configurations (Fig. 3). Supply conditions were controlled and could be adapted. The simplified model setup differs from a real situation where air can move freely through the room. This confinement, in combination with the assumed velocities of the contaminated airflow, is considered a conservative approximation of the real OT situation.

Both measurements and CFD simulations were performed to assess the air quality improvement, compared to a situation without the use of the ventilation configuration, i.e. no clean air provision near the wound. Particle concentration was applied as the main evaluation attribute [38]. Particle concentrations were assessed in the center of the wound area, at 0.12 m height (measurements; CFD) and near the wound (CFD). The parameter analysis performed with the two methods is summarized in Table 1. In the measurement series the velocity of the HEPA filtered airflow (V_{HEPA}) and the velocity of the contaminated flow (V_{cont}) were varied for both isothermal and non-isothermal situations. All possible combinations were investigated: 40 cases for Configuration 1; 30 cases for Configuration 2. For the CFD analysis, a base case was defined for both configurations ($\Delta T_{\text{HEPA-cont}} = 0$ K, $V_{\text{cont}} = 0.30$ m/s, $I_{\text{cont}} = 1\%$, $V_{\text{HEPA}} = 0.10$ m/s, $I_{\text{HEPA}} = 5\%$). In the CFD analysis sensitivity of individual parameters was investigated one by one, in each case departing from the base case: 14 cases for Configuration 1; 13 cases for Configuration 2. This limitation was based on simulation and analysis time required. Finally, in the CFD analysis the effect of a heat flux from the wound (45.5 W/m²) was investigated as well. A more detailed description of the measurement setup and simulation model is given in the following two subsections.

2.1.1. Measurements

Particles of size 0.5–0.7 μm were measured in the center of the wound at 0.12 m height by a 1 l/min particle counter (5% accuracy; Lighthouse, Remote 2014). A second similar particle counter monitored the particle concentration of the contaminated airflow as function of time. This air was taken from an adjacent large room with relatively constant controlled conditions. The HEPA-filtered air temperature was controlled by a sensor within the supply duct which was connected with the air heater, for the cooling cases outdoor air was used and reheated; the temperature of the contaminated airflow was not controlled.

The particle size, as applied, does not agree with the typical particle size as can be expected for CFUs. Scaltriti et al. [39] contend that skin debris usually ranges between 2.5 and 20 μm and that approximately 5–10% of skin debris carry bacteria. Noble et al. [40] found that micro-organisms associated with human disease were usually found on particles in the range of 4–20 μm. The transfer of particles through the air mainly depends on the particle size. While large particles will sediment earlier by gravity, small particles can be transferred over large distances through the air [41,42]. As settling velocity is higher and deposition is faster for larger

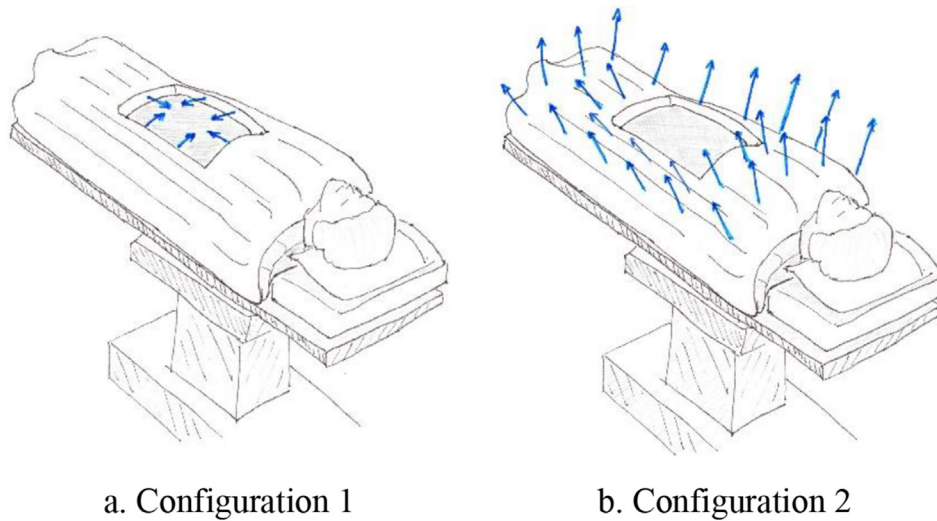


Fig. 1. Configurations of a local ventilation device with clean air supply around and parallel to the wound area (a. Configuration 1) and clean air supply from the top surface of the blanket (b. Configuration 2). Blue arrows indicate the direction of the clean air supply (Figures based on 3M [36]). (For interpretation of the references to colour in this figure legend, the reader is referred to the web version of this article).

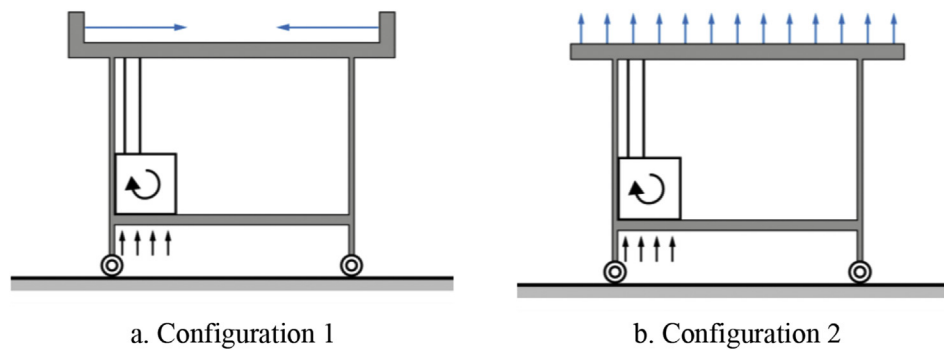


Fig. 2. Configurations of the instrument table with clean air supply around and parallel to the table surface (a. Configuration 1) and clean air supply from the top surface of the table (b. Configuration 2). Blue arrows indicate the direction of the clean air supply. (For interpretation of the references to colour in this figure legend, the reader is referred to the web version of this article).

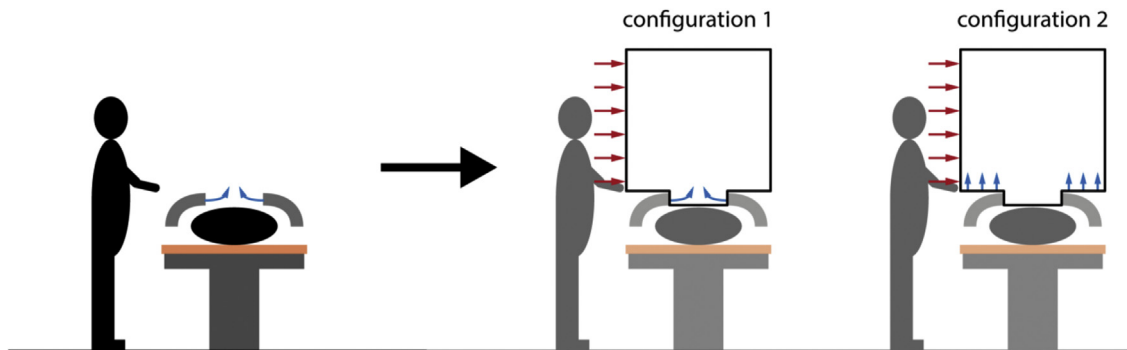


Fig. 3. Origin of the simplified representation for the parameter study. The geometry represents the wound area with a contaminated airflow [red arrows] coming from the side of the surgeon and HEPA-filtered air [blue arrows] supplied near the wound area (Configuration 1) or from the top surface of the blanket (Configuration 2). (For interpretation of the references to colour in this figure legend, the reader is referred to the web version of this article).

particles, location of the source becomes an important parameter in the analysis. So, selection of assessment cases and assessment itself (experimental and numerical) will be more tedious. For particles in the order of $10\ \mu\text{m}$, the settling velocity is much smaller. Earlier research [7] concluded that for clean room situations, up to particle

sizes of around $10\ \mu\text{m}$, the particle behavior (e.g., due to drag and gravitational force) is comparable to smaller particles (or gas). Referring to the average air velocities present in the simplified representation, the test set-up as applied has conditions similar to a cleanroom situation. Therefore the measurements were restricted

Table 1

Summary of parameter analyses performed (C1: Configuration 1; C2: Configuration 2; $\Delta T_{\text{HEPA-cont}} = T_{\text{HEPA filtered flow}} - T_{\text{contaminated flow}}$; V_{cont} : velocity contaminated flow; V_{HEPA} : velocity HEPA filtered flow; I_{HEPA} : turbulence intensity supply HEPA filtered flow; N/A = not applicable). Bold italic indicates the base case for the CFD study.

Analysis type	$\Delta T_{\text{HEPA-cont}}$	V_{cont} [m/s]	V_{HEPA} [m/s]	I_{HEPA} [%]
Measurement	C1: 0/+22	C1: 0.1/0.3/0.5/0.7/0.9	C1: 0.1/0.2/0.3/0.4	N/A
	C2: -5/0	C2: 0.1/0.3/0.5/0.7/0.9	C2: 0.1/0.2/0.3	
CFD	C1: 0 /+16/+22	C1: 0.1/ 0.3 /0.5/0.7/0.9	C1: 0.1 /0.2/0.3/0.4	C1: 5/15/25/35/45
	C2: -5/ 0 /+3	C2: 0.1/ 0.3 /0.5/0.7/0.9	C2: 0.1 /0.2/0.3	C2: 5/15/25/35/45

to 0.5–0.7 μm particle sizes.

Additionally, in the laboratory set-up a statistical comparison was made for different particle sizes present in the contaminated air. The particle sizes 0.5–0.7 μm , 0.7–2.5 μm , 2.5–10 μm and >10 μm were measured for each case investigated. The results for the particle size 0.5–0.7 μm were compared to the other particle sizes using paired t-tests (two-tailed), at a 5% significance level. From these analyses no significant differences between particle size 0.5–0.7 μm and the other particle sizes were found, both for Configuration 1 ($p > 0.10$) and Configuration 2 ($p > 0.24$). Only the particle size >10 μm showed a significant difference ($p = 0.02$) for a HEPA-filtered air velocity of 0.10 m/s, in Configuration 1. Moreover, the trend of the results were similar for all particle sizes for both concepts. Therefore, only the results of particle sizes 0.5–0.7 μm are presented. Particle characteristics of the contaminated air were not investigated. Aspect ratios in the order of 1 and a density in the order of 1000 kg/m^3 were assumed.

Fig. 4 presents the time line of one measurement series consisting of three transition periods and three periods from which data was used in the analysis. The measurement series is designed in this way to calculate the relative particle concentrations (Equation (1)):

$$\text{Relative particle concentration} = (\text{median}C_{\text{clean}(B)} / \text{median}C_{\text{contaminated}(A+B)}) * 100\%, \quad (1)$$

In Eqn. (1), the median of the particle concentration in the period with clean air ventilation (B; see Fig. 4) is divided by the median of the particle concentration in the periods with contaminated airflow only (A and C), to obtain a percentage. Statistical software [43] was used for analysis of the experimental results. The reproducibility was evaluated by comparison of two series of 15 samples of 30 s (i.e. 0.5 l) by the Wilcoxon matched-pairs test (two-tailed). The two measurement series were performed on different days. Next to this, different situations were compared by the one-tailed paired t-test ($N = 30$). P-values of <0.05 were considered as significant.

Minimum air change rate for the box, assuming the contaminated flow rate, in all cases investigated was in the order of 300 h^{-1} . The contaminated-only part of the measurement series (indicated with A and C) were measured to acknowledge any potential change in the contamination concentration. In addition, different measurement days showed differences in the absolute particle concentration present in the contaminated air.

2.1.2. Simulations

ANSYS Fluent [44] version 14.5 was used as simulation software for the CFD-simulations. The model investigated assumed the same

simplified representation as was applied for the experimental model. For the supply boundary conditions, a uniform profile was prescribed for the velocity and turbulence at the supplies (see Table 1). The outlet was modeled as pressure outlet with $I_{\text{outlet}} = 5\%$ (0.1 m characteristic length) in case backflow occurred. For non-isothermal cases, the walls are assumed adiabatic, while fixed temperatures were set for the contaminated and clean air supply. Contaminants were modeled as passive scalar [7,45], not as individual particles. A User Defined Scalar (UDS) was defined with an updated term for isotropic diffusivity to model the contamination [44]. Boundary conditions for the UDS of the contaminated air were set as 1 [-] and of the clean air as 0 [-]. At the walls a zero flux is assumed.

A validation study (including grid sensitivity study and turbulence model selection) was conducted prior to the parameter analysis. For that, validation measurements were performed at 34 positions in the simplified representation. The largest gradients of the measured quantities were expected close to the wound area. For this reason the measurement positions were concentrated at these locations. Airflow measurements were performed by a hot sphere anemometer (Sensor-Electronic, type SensoAnemo 5132SF) with an accuracy of ± 0.02 m/s + 1.5% of the readings. The air velocity was measured for a period of 3 min on each position with a sampling frequency of 10 Hz in order to capture sufficient flow characteristics and obtain sufficient data [46]. Due to the thermal inertia of the hot sphere anemometer, damping of the air velocity fluctuation occurs. This results in an underestimation of the turbulence intensity [47]. The accuracy with which the turbulent kinetic energy can be derived is therefore constrained.

The grid sensitivity analysis was performed by creating a factor 2 coarser grid and a factor $\sqrt{2}$ finer grid (Coarse: 182,250 cells; Middle: 1,458,000 cells; Fine: 4,000,752 cells). The grids were compared quantitatively on 34 points comparable to the approach used by Van Hooff and Blocken [48]. The parameters used for comparison are the mean air velocity (U [m/s]) and turbulent kinetic energy (k [m^2/s^2]) respectively. The relative error between the middle and fine grid, for U and k respectively, were 2% and 101% for Configuration 1 and 2% and 44% for Configuration 2. Although the relative error for the turbulent kinetic energy (k) is large, Fig. 5 illustrates that absolute differences are very small, in particular close to the wound surface (i.e. lower side of the model). The middle grid was assessed acceptable for the purpose of this research, considering the accuracy of the model and the resolution of the grid (For the most important surface areas (blanket and wound area) the maximum y^+ -value is 1.4 [Configuration 1] and 1.6 [Configuration 2]).

For the turbulence model selection, validation measurement data for mean air velocity, turbulent kinetic energy and

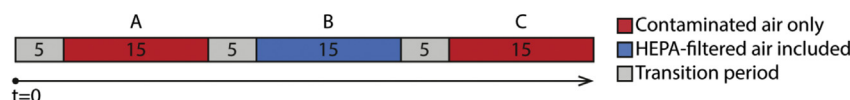


Fig. 4. Illustration of the time laps of the measurement series. The numbers indicate the number of measurement samples per period (30 s/sample).

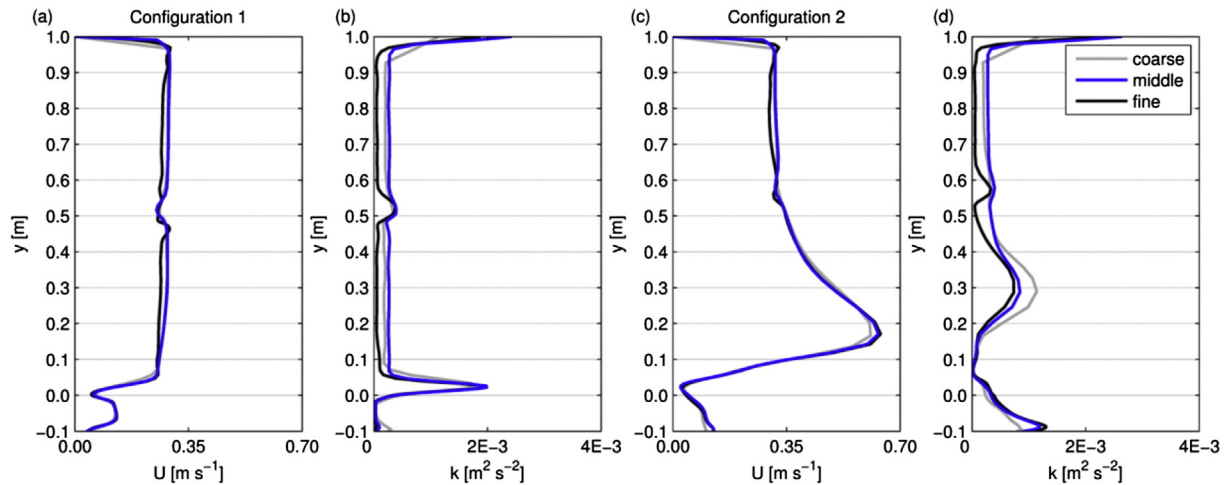


Fig. 5. Mean air velocity (U) and turbulent kinetic energy (k) at line $(x, z) = (0.4, 0.5)$ for the coarse, middle and fine grid of Configuration 1 (a–b) and Configuration 2 (c–d). The y -axis represents the height of the model. (Boundary conditions: C1: $V_{\text{HEPA}} = 0.13$ m/s, $I_{\text{HEPA}} = 4\%$, $V_{\text{cont}} = 0.36$ m/s, $I_{\text{cont}} = 1\%$; C2: $V_{\text{HEPA}} = 0.11$ m/s, $I_{\text{HEPA}} = 2\%$, $V_{\text{cont}} = 0.36$ m/s, $I_{\text{cont}} = 1\%$).

temperature were used. Performance of several RANS-models (standard k - ϵ , Realizable k - ϵ , RNG k - ϵ , Low-Reynolds [44], SST k - ω , Reynolds Stress Model [RSM]) was compared for the fine grid resolution, including low-Reynolds near wall treatment [44]. Large Eddy Simulation was not considered due to computational costs [49].

The RSM model showed the best and most stable overall performance. For this reason the RSM model was applied as turbulence model for the parameter study. Compared to the experimental data from the validation measurements, the mean relative error on the mean air velocity (U) was $\leq 10\%$ in both isothermal and non-isothermal conditions. For the temperature (T) the mean relative error was $\leq 5\%$. The mean relative error on turbulent kinetic energy (k) was respectively 72% and 94% for the isothermal and non-isothermal situation. This difference is also attributed to the velocity measurement technique applied [47]. Simulation results for the relative particle concentration distribution have also been compared to the measurements. This is explained below and discussed further in Section 3.1.

In the CFD-analysis the relative particle concentration is calculated as follows (Equation (2)):

$$\text{Relative particle concentration} = (\Gamma_{\text{clean}}/\Gamma_{\text{contaminated}}) * 100\%, \quad (2)$$

where $\Gamma_{\text{contaminated}}$ is the scalar value for the case without HEPA filtered air supply. By definition then, $\Gamma_{\text{contaminated}} = 1$. Γ_{clean} is the scalar value for the case with HEPA filtered air supply. The simulated relative particle concentration was compared to the measured results (centrally located measurement position at 0.12 m height from the wound area). The average difference in relative particle concentration between the simulation data and the median of the measurement results was 19% for Configuration 1 and 3% for Configuration 2. For Configuration 1, near the measurement location a high gradient was simulated for the relative particle concentration. This may explain the larger difference found. Nevertheless, the trend in the data for the different boundary conditions was similar. For this reason, the performance of the UDS model was assumed sufficient for both configurations.

As the measurement set-up had limitations for assessing the relative particle concentration close to the wound area, CFD-results were applied for this analysis. In this case the relative particle

concentration was determined in the cell-layer just above the wound. The volume-weighted scalar value was applied for that. It is assumed that this value provides a representation of the potential deposition of particles near the wound. The approach chosen, however, does not reflect actual particle deposition as a scalar was used for the analysis. To avoid any confusion this indicator is addressed as the *volume-weighted average relative particle concentration* near the wound area.

In the CFD simulations the SIMPLE algorithm has been applied to solve the equations. Steady-state simulation was applied for all cases. In a post-processing step the contamination distribution was calculated with the User Defined Scalar (UDS), assuming a fixed flow field for velocity and temperature. Pressure interpolation was of second order and second order discretization schemes were used for both convection terms and viscous terms. The Boussinesq approximation was applied to consider the buoyancy effect. Convergence was assumed to be obtained when the residuals leveled off and residuals reached a level of 10^{-3} for x , y and z momentum, k , ϵ , continuity and the User Defined Scalar (UDS) and 10^{-6} for energy. Furthermore, convergence was checked on a position 0.12 m above the wound in the center of the model, at which the particle model was validated by measurements. Convergence was assumed to be obtained when fluctuations in the air velocity (m/s) and relative particle concentration (%) were less than 0.01 m/s and 0.1%, respectively.

2.2. Full-scale prototype in-situ assessment

In addition to the simplified representation, the performance of prototypes of the local ventilation system was explored in a detailed full-scale mock-up of an operating theater (OT; $6 \times 7 \times 3$ m). The OT has been built for demonstration purposes only. Prototypes were developed for the ventilating blankets and the instrument table (Fig. 6). The prototypes of the ventilating blankets were hand-made from air mattresses and permeable cloth (325 $[\text{m}^3/\text{h}]/\text{m}^2$ at 120 Pa; the dimensions of the wound area were $0.60 \times 0.40 \times 0.07$ m (L x W x H), resembling operating dimensions of common active warming devices). The surface area of the prototype of the ventilating instrument table measured 0.80×0.60 m (L x W). For both configurations clean HEPA-filtered air (H14 filter class) was supplied to the blanket and the instrument table.

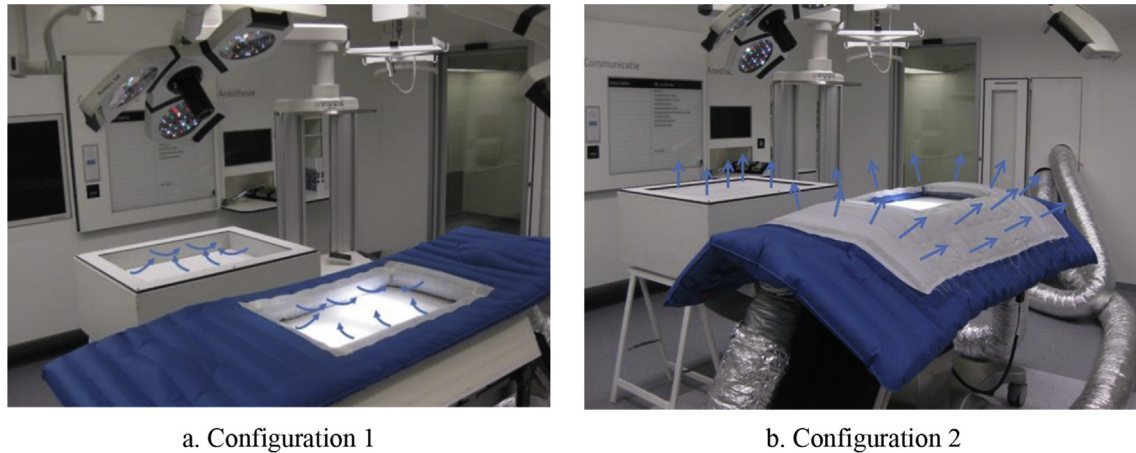


Fig. 6. Full-scale test setup of the ventilating blanket and instrument table for both configurations in the operating theater mock-up of the OT. The arrows represent the HEPA filtered airflows.

Both blanket configurations were positioned on a self-made dummy patient on the operating table, put at the center of the OT. The instrument table was placed at 0.5 m from and parallel to the long side of the operating table. The instrument tabletop and the topside of the dummy were positioned at 1.15 m height.

According to the Dutch guideline VCCN RL7 [50] the measurements were performed in an at-rest situation, without people in the OT. The operating lamps were turned on and positioned above the operating table, as prescribed in the guideline. The main OT ventilation system present in the facility was capable of arriving at very low relative particle concentrations under standard conditions (ultraclean). As a result the effect of the local system would be obscured. Therefore, no additional ventilation was assumed in the OT and the fans for the local ventilation devices were placed outside the OT. Air flow rate balance was obtained by distributed overflow openings in the OT. The air flow rates applied resulted in an air change rate of 4.8 h^{-1} for Configuration 1 and 11.4 h^{-1} for Configuration 2. In a normal situation with a UDF system, fresh air change rates would add up to the order of 20 h^{-1} , and, with recirculation, up to 80 h^{-1} for large plenums ($3 \times 3 \text{ m}$) as currently applied in practice. The effect of possible disturbance by the main OT ventilation therefore is not included in the applied full-scale test procedure. However, the results from the simplified representation provide information on the sensitivity towards such type of disturbance.

V_{HEPA} for the table as well as the blanket was 0.40 m/s and 0.30 m/s for Configuration 1 and Configuration 2 respectively. These velocities were derived from the parameter analysis of the simplified representation of the device. The clean air supply temperature of the blanket in case of Configuration 1 was set at $37 \text{ }^\circ\text{C}$. This is based on normally applied supply temperatures in active warming devices to control the body temperature of the patient [14]. As the room temperature in the OT was not controlled, the resulting air temperature difference with the surroundings was limited to 11 K. The supply temperature for the instrument table in this case was set isothermal. For Configuration 2 isothermal conditions were assumed for both the blanket and the instrument table.

2.2.1. Measurement protocol

In accordance with [50], the in-situ performance of the local ventilation system prototypes was assessed by particle measurements ($\geq 0.5 \text{ }\mu\text{m}$). The relative particle concentration was derived by comparing the particle concentration in the wound area to a

reference point in the contaminated periphery (protection class). Furthermore, smoke tests were conducted to visualize the airflows.

The conventional measurement setup is based on one large clean area around the instrument tables, wound area and operating team, as depicted in Fig. 7a. This setup aligns with an assumed UDF OT ventilation system. In our case the main OT ventilation system (in fact a UDF) was shut off, only the local ventilation systems (blanket and instrument table) were operated. As the local ventilation systems create two smaller clean areas in the OT, the VCCN guideline was modified to account for this. Fig. 7b shows the modifications of the measurement setup for the ventilating blanket of Configuration 1. The measurement setup for the instrument table was similar to the blanket. The measurement positions were moved to the clean area of the table. In addition to the measurement positions prescribed in the guideline, a point was added in between the blanket and the instrument table to measure the air quality at the surgeon's position (C_s).

The protection class measurements of the instrument table and blanket were performed separately, where each corner of the clean area was measured individually ($N = 30$). A reference measurement point in the periphery ($C_p\#$) was positioned at 1.5 m from the particle source (Emission#). The particle source (Atomizer Aerosol Generator, ATM 226) regularly dispersed particles to approximately 15,000,000 particles per m^3 in the periphery with a particle size of $0.5 \text{ }\mu\text{m}$ (more than 90% in range $0.3\text{--}1.5 \text{ }\mu\text{m}$; assumed aspect ratio in the order of 1). The other particle counters were placed at the corner ($C_c\#$) and in the middle (C_m) of the wound area and one at the surgeon's position (C_s). The particle emission was placed at 1.5 m height, the particles were counted at 1.2 m height by 2.83 L/min particle counters (2.5% accuracy; Lighthouse, Remote 3016). At the surgeon's position a 28.3 L/min particle counter was used (2.5% accuracy Lighthouse, Solair+ 3100). The particle counters at the four positions counted at the same time every minute.

2.2.2. Data analysis

As the lay-out of the full-scale prototype in-situ assessment differs from the simplified representation, also the particle measurement procedure and the calculation of the relative particle concentration was adapted accordingly. The relative particle concentration was calculated by comparing $C_c\#$, C_m and C_s with the measured particle concentration in the periphery ($C_p\#$). The four particle concentrations were measured simultaneously for 20 min, where the first 5 min were used as transition period. Therefore, the

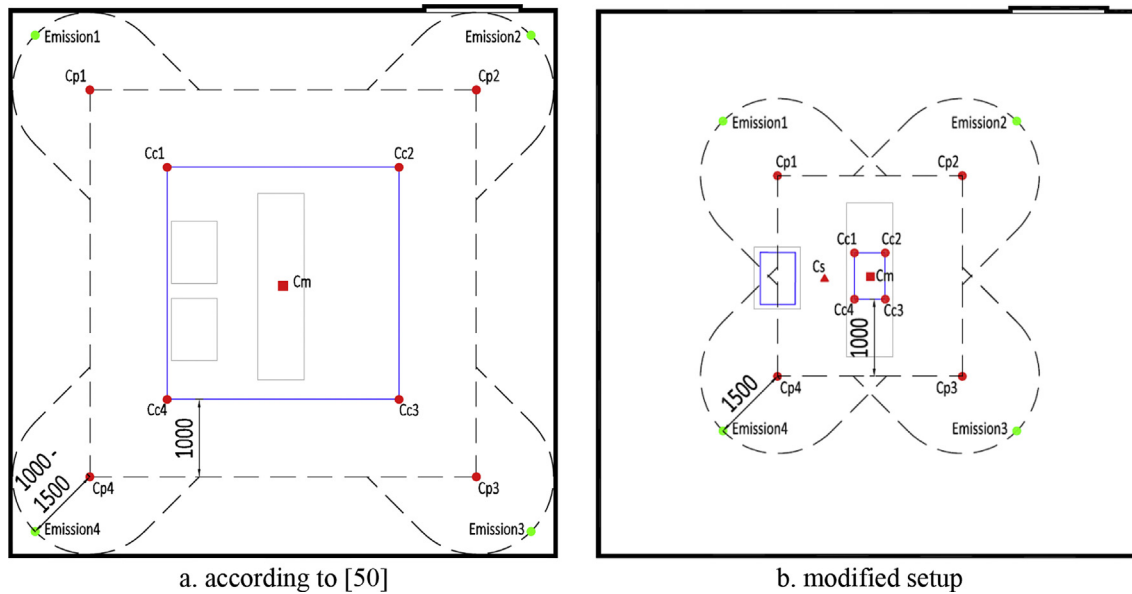


Fig. 7. Measurement setup according to [50], based on one large clean area (a.) and the modification regarding the ventilating blanket of Configuration 1 (b.). The solid (blue) squares visualize the clean areas, the emission positions are green. The points represent the measurement position of the particle concentration in the periphery (Cp#), corner (Cc#), middle (Cm) and surgeon (Cs) and the position where particles are emitted (Emission#). The values indicate the distance in [mm]. (For interpretation of the references to colour in this figure legend, the reader is referred to the web version of this article).

relative particle concentration was determined from 15 measurements of 1 min each:

$$\text{Relative particle concentration} = \text{Median}(C_x/C_{p\#}) * 100\%, \quad (3)$$

where C_x is the particle concentration measured at Cc#, Cm or Cs in particles/m³ and $C_{p\#}$ is the particle concentration, in particles/m³, measured in the periphery at the corner under investigation. The median was used because not all series showed a normal distribution. In order to determine the reproducibility, each measurement series was performed a second time on another day.

Statistical software [43] was used for the data analysis. The reproducibility was evaluated by comparison of the two series of 15 samples by the Wilcoxon matched-pairs test (two-tailed). The different configurations were compared by the one-tailed paired t-test ($N = 30$). P-values of <0.05 were considered as significant.

3. Results and discussion

The analysis of the ventilation performance of the new devices has been conducted in two consecutive steps: 1. Simplified representation; 2. Full-scale mock-up test. Therefore, the results and discussion are presented separately for both steps as well. An overall discussion will combine the outcomes.

3.1. Simplified representation

The measurement and simulation results at the measurement position for Configuration 1 for both the isothermal and non-isothermal series are shown in Tables. 2 and 3 respectively. The results indicate that a higher supply velocity of the filtered airflow V_{HEPA} significantly reduces the measured relative particle concentrations ($p < 0.04$). Comparison of the isothermal to the non-isothermal case ($\Delta T_{\text{HEPA-cont}} = 22 \text{ K}$) results in significantly higher measured relative particle concentrations for the non-isothermal situation ($p < 0.04$). A higher supply temperature of the HEPA-filtered airflow negatively influences the performance of Configuration 1.

The results of the isothermal situation for Configuration 2 are summarized in Table. 4. No significant differences were observed for different velocities of the HEPA-filtered airflow ($p < 0.17$). This illustrates that all evaluated velocities of the filtered airflow yield similar results. The non-isothermal situation ($\Delta T_{\text{HEPA-cont}} = -5 \text{ K}$) is presented in Table. 5 and showed no significant differences compared to the isothermal situation. This indicates that a 5 K lower temperature of the filtered airflow does not affect the performance of the ventilation device.

The CFD results for Configuration 1 show a higher efficiency when compared to the measurement results. They approach the low range values as measured for the different HEPA-filtered air flow velocities. For Configuration 2, the results are in line with the outcomes from the measurements. The measurement results assume a better performance for Configuration 2. The CFD results only assume this at $V_{\text{HEPA}} = 0.1 \text{ m/s}$.

Fig. 8 demonstrates that in the CFD analysis, for both configurations, a layer of clean air is calculated around the wound. The sensitivity to the measurement position was investigated by comparing the CFD-results to the measurement results if the location differed in height by $\pm 0.01 \text{ m}$ (see Tables. 2–5). For Configuration 1 the average difference between measured and simulated relative particle concentration for all simulated cases was 19% at the measurement position, 10% at $+0.01 \text{ m}$ above the measurement position and 27% at -0.01 m below the measurement position. For Configuration 2 this average difference for all cases was 2.9% at the measurement position, 2.6% at $+0.01 \text{ m}$ above the measurement position and 3.2% at -0.01 m below the measurement position. For Configuration 1 the sensitivity to the measurement location is obvious.

In Configuration 2, contaminated air is pushed upward but apparently can be captured in a recirculating eddy near the wound. This might explain the non-significant differences as measured for different velocities of the filtered airflow and simulated results for the volume-weighted average relative particle concentration near the wound area (Fig. 9a). Considering a velocity of 0.10 m/s for the filtered airflow and a velocity of 0.30 m/s for the contaminated airflow this concentration was 0% and 3% for Configuration 1 and 2 respectively.

Table 2

Measurement and simulation results for the isothermal cases for Configuration 1 (central point at 0.12 m from wound area). Measurement values are median (range) of the relative particle concentration [%] for particles sized 0.5–0.7 μm measured in the wound area ($N = 30$). V_{cont} = air velocity of the contaminated airflow [m/s], V_{HEPA} = air velocity of the HEPA-filtered airflow [m/s]. CFD values are at the measurement position (–0.01 m, +0.01 m).

	V_{cont} [m/s]					V_{cont} [m/s]
	0.10	0.30	0.50	0.70	0.90	0.30
V_{HEPA} [m/s]	Measurement					CFD
0.10	12 (0–94)	43 (15–84)	66 (57–74)	69 (63–78)	77 (67–86)	12 (4, 26)
0.20	1 (0–3)	12 (1–24)	30 (21–43)	49 (36–59)	63 (56–72)	0 (0, 0)
0.30	1 (0–3)	2 (0–11)	12 (7–15)	17 (10–23)	35 (29–44)	0 (0, 0)
0.40	0 (0–4)	0 (0–3)	1 (0–3)	7 (4–12)	11 (9–14)	0 (0, 0)
V_{HEPA} [m/s]	CFD					
0.10	0 (0, 0)	12 (4, 26)	32 (11, 53)	46 (26, 64)	55 (36, 72)	

Table 3

Measurement and simulation results for the non-isothermal cases for Configuration 1 ($\Delta T_{\text{HEPA-cont}} = +22$ K; central point at 0.12 m from wound area). Measurement values are median (range) of the relative particle concentration [%] for particles sized 0.5–0.7 μm measured in the wound area ($N = 30$). V_{cont} = air velocity of the contaminated airflow [m/s], V_{HEPA} = air velocity of the HEPA-filtered airflow [m/s], N/A = not applicable. CFD values are at the measurement position (–0.01 m, +0.01 m).

	V_{cont} [m/s]					V_{cont} [m/s]
	0.10	0.30	0.50	0.70	0.90	0.30
V_{HEPA} [m/s]	Measurement					CFD
0.10	86 (73–100)	97 (88–100)	89 (75–100)	78 (69–93)	81 (73–95)	62 (55, 70)
0.20	58 (29–73)	91 (83–100)	80 (70–90)	73 (61–87)	75 (70–88)	N/A
0.30	17 (1–44)	60 (43–72)	61 (48–72)	59 (44–74)	55 (49–68)	N/A
0.40	0 (0–4)	6 (3–9)	30 (22–38)	31 (27–45)	47 (39–58)	N/A

Table 4

Measurement and simulation results for the isothermal cases for Configuration 2 (central point at 0.12 m from wound area). Measurement values are median (range) of the relative particle concentration [%] for particles sized 0.5–0.7 μm measured in the wound area ($N = 30$). V_{cont} = air velocity of the contaminated airflow [m/s], V_{HEPA} = air velocity of the HEPA-filtered airflow [m/s]. CFD values are at the measurement position (–0.01 m, +0.01 m).

	V_{cont} [m/s]					V_{cont} [m/s]
	0.10	0.30	0.50	0.70	0.90	0.30
V_{HEPA} [m/s]	Measurement					CFD
0.10	0 (0–2)	0 (0–2)	0 (0–4)	1 (0–6)	17 (8–21)	1 (1, 1)
0.20	0 (0–2)	0 (0–1)	0 (0–3)	0 (0–4)	1 (0–4)	0 (0, 0)
0.30	0 (0–3)	0 (0–5)	0 (0–1)	0 (0–3)	1 (0–2)	0 (0, 0)
V_{HEPA} [m/s]	CFD					
0.10	0 (0, 0)	1 (1, 1)	3 (4, 3)	12 (12, 11)	23 (24, 23)	

Table 5

Measurement and simulation results for the non-isothermal cases for Configuration 2 ($\Delta T_{\text{HEPA-cont}} = -5$ K; central point at 0.12 m from wound area). Measurement values are median (range) of the relative particle concentration [%] for particles sized 0.5–0.7 μm measured in the wound area ($N = 30$). V_{cont} = air velocity of the contaminated airflow [m/s], V_{HEPA} = air velocity of the HEPA-filtered airflow [m/s]. CFD values are at the measurement position (–0.01 m, +0.01 m).

	V_{cont} [m/s]					V_{cont} [m/s]
	0.10	0.30	0.50	0.70	0.90	0.30
V_{HEPA} [m/s]	Measurement					CFD
0.10	0 (0–3)	0 (0–3)	0 (0–2)	1 (0–1)	8 (5–11)	1 (1, 1)
0.20	1 (0–3)	0 (0–5)	0 (0–1)	1 (0–3)	1 (0–6)	N/A
0.30	1 (0–2)	1 (0–2)	1 (0–4)	0 (0–1)	0 (0–2)	N/A

For the measurements, in approximately 75% of the cases a significant difference between the first and second measurement series of 15 samples for Configuration 1 was found. For Configuration 2 no significant differences were reported between the two series. Reproducibility for Configuration 1 measurements therefore was low. This effect may be explained by the fact that approximately 7 times less filtered air was supplied in Configuration 1 compared to Configuration 2. Furthermore, the measurement position in Configuration 1 was close to the boundary between the clean air layer and the contaminated air layer (Fig. 8a). A small difference in the position of this boundary can quickly result in

large differences for the relative particle concentration. For practical reasons the measurement location had to be kept in place.

The effect of simulated variations in the boundary conditions for the supply velocity, turbulence intensity and temperature of the filtered airflow on the volume-weighted average relative particle concentration near the wound area is shown in Fig. 9. For isothermal conditions, Configuration 1 shows a constant value of 0% for the different boundary conditions investigated. For Configuration 2 a higher supply velocity up to 0.30 m/s improves the performance, i.e. a lower volume-weighted average relative particle concentration near the wound area. On the other hand, increasing

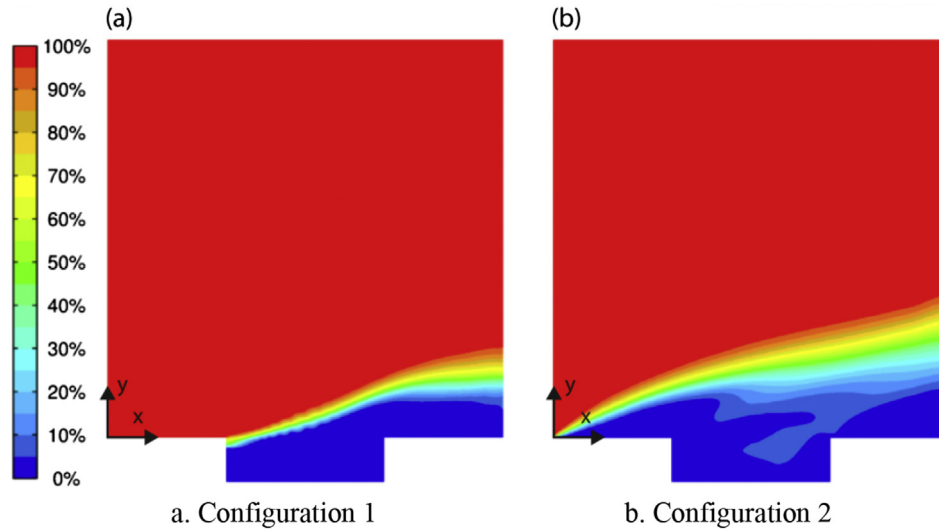


Fig. 8. Concentration field of the relative particle concentration at section $z = 0.4$ m for (a) Configuration 1 and (b) Configuration 2 ($V_{\text{HEPA}} = 0.1$ m/s; $V_{\text{cont}} = 0.3$ m/s; isothermal).

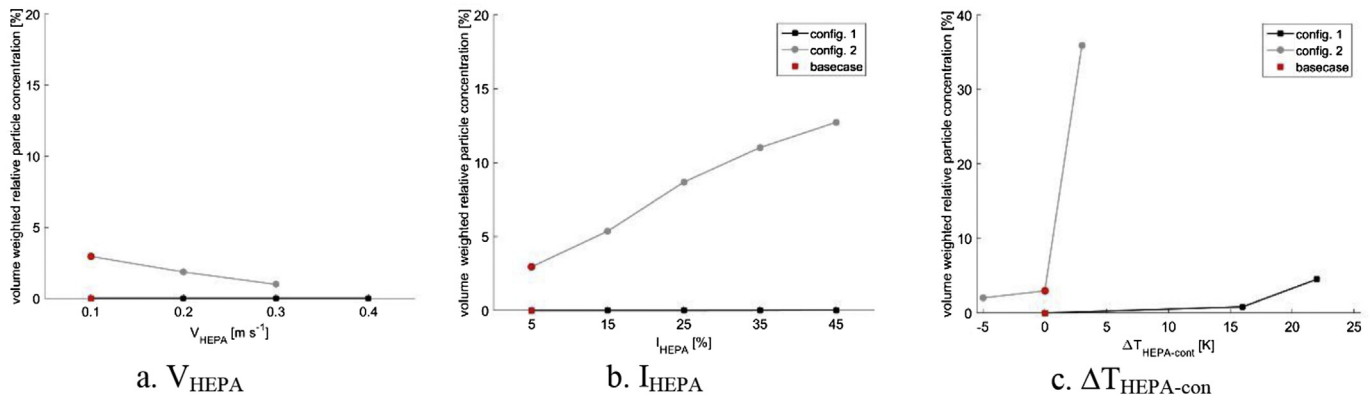


Fig. 9. Simulated volume-weighted average relative particle concentration near the wound area as a function of (a) V_{HEPA} , (b) I_{HEPA} , and (c) $\Delta T_{\text{HEPA-cont}}$. Each graph assumes base case conditions for the other non-varying variables ($V_{\text{cont}} = 0.30$ m/s).

the turbulence intensity for Configuration 2 increases this value almost linearly to 13%.

Both configurations show an increment when $\Delta T_{\text{HEPA-cont}} > 0$ K (Fig. 9c). This effect is explained from an increased mixing for both configurations. As an example, Fig. 10 shows the temperature profile and the relative particle concentration for $\Delta T_{\text{HEPA-cont}} = +22$ K situation, for Configuration 1. The temperature gradient near the wound area in this case correlates with the increased volume-weighted average relative particle concentration near the wound area because of the induction of contaminated air into the HEPA ventilated wound space (refer to Fig. 8a). For $\Delta T_{\text{HEPA-cont}} = -5$ K (Configuration 2) the protective layer around the wound is improved and the value is reduced to 2%. Finally, the effect of a thermal plume from the wound did not affect the relative particle concentration near the wound.

3.2. Full-scale prototype in-situ assessment

Tables 6 and 7 show the results of the full-scale measurements for Configuration 1 and 2 respectively. The measurement positions have been indicated in Fig. 7. The results are listed for both series separately because series 1 and 2 yielded mostly significant differences per measurement position. For the

instrument table of Configuration 2, only one measurement series was conducted.

For Configuration 1, significant differences were found between the series for most measurement positions, probably caused by imperfections of the hand-made prototype. Smoke tests showed these imperfections: Fig. 11a shows the turbulent clean air supply from the long side of the blanket, compared to the short side of the blanket (Fig. 11b). Especially corner 4 showed varying results caused by the internal structure of the blanket. The blanket of Configuration 2 also yielded mostly significant differences between the two series. Entrapment of contaminants in a local eddy above the wound area caused a high range of relative particle concentrations at the middle position (Fig. 11c). Corner 4 showed low relative particle concentrations compared to the other corner positions. This corner in the prototype was curved, resulting in a smaller distance of the clean air supply to the particle monitor position. The instrument table prototypes for both configurations yielded more uniform results compared to the blankets. This most probably is caused by the better controlled distribution and unidirectional airflow that could be obtained for these prototypes compared to the blankets (Fig. 11d,e,f). The instrument table of Configuration 2 showed a relative particle concentration of 0.0% at the middle position for all measurements, which was the best

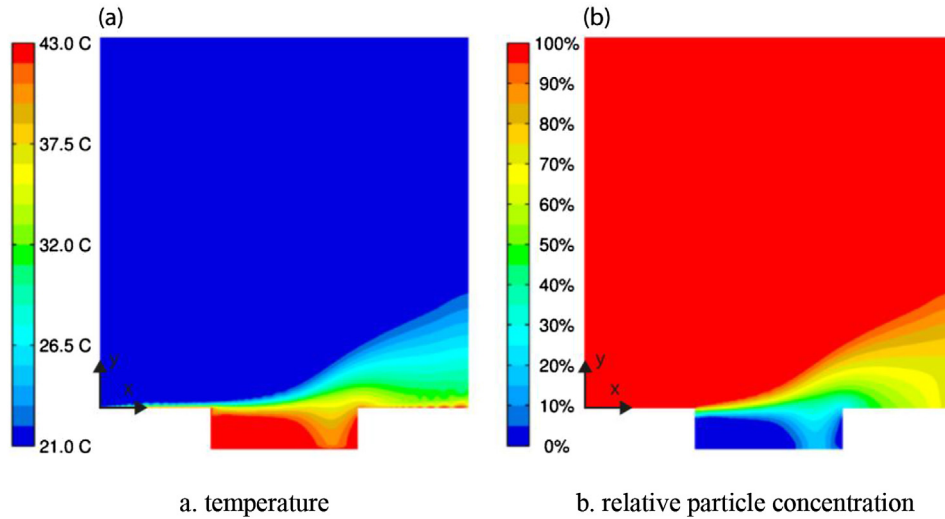


Fig. 10. Results of Configuration 1 with $\Delta T_{HEPA-cont} = +22$ K, (a) temperature profile at section $z = 0.4$ m and (b) relative particle concentration at section $z = 0.4$ m.

Table 6

Configuration 1: Median (range) of the relative particle concentration [%] for particles $\geq 0.5 \mu m$ ($N = 15$). Measurement positions are shown in Fig. 7. The medians (range) of the four positions together are given in bold ($N = 60$).

Position	Blanket Series 1	Blanket Series 2	Table Series 1	Table Series 2
C_{corner}	0.4 (0.0–4.3)	0.5 (0.0–26.6)	1.8 (1.0–4.6)	0.8 (0.4–1.9)
C_{c1}	0.5 (0.4–0.7)	0.0 (0.0–0.0)	2.0 (1.2–3.3)	0.5 (0.4–0.6)
C_{c2}	0.4 (0.1–1.0)	0.3 (0.0–0.7)	2.4 (1.1–4.6)	0.6 (0.4–1.1)
C_{c3}	0.0 (0.0–0.1)	0.5 (0.4–0.8)	1.4 (1.0–1.8)	1.3 (0.7–1.9)
C_{c4}	2.6 (0.6–4.3)	18.8 (14.0–26.6)	1.7 (1.1–2.2)	1.2 (1.0–1.8)
C_{middle}	5.0 (1.0–10.5)	0.9 (0.2–6.7)	1.7 (0.5–3.1)	0.7 (0.3–1.9)
C_{m1}	7.7 (4.8–10.5)	2.6 (1.6–6.7)	2.2 (1.4–3.1)	0.6 (0.3–0.9)
C_{m2}	2.9 (1.6–7.1)	0.5 (0.2–1.8)	1.9 (1.0–2.6)	0.6 (0.3–1.1)
C_{m3}	2.6 (1.3–5.4)	0.8 (0.5–1.5)	0.7 (0.5–0.8)	0.6 (0.5–0.9)
C_{m4}	6.6 (1.0–10.2)	0.8 (0.4–1.3)	1.7 (1.2–2.1)	1.1 (0.9–1.9)
$C_{surgeon}$	43.9 (3.4–100)	64.8 (6.8–100)	60.6 (18.8–100)	37.1 (11.0–90.0)
C_{s1}	100 (81.7–100)	100 (79.9–100)	100 (66.6–100)	20.8 (13.4–37.1)
C_{s2}	14.3 (3.4–41.4)	22.1 (6.8–44.2)	56.8 (23.2–73.6)	37.8 (25.3–52.4)
C_{s3}	16.9 (5.9–28.9)	81.9 (58.4–100)	34.8 (18.8–48.4)	31.6 (11.0–42.4)
C_{s4}	79.3 (46.3–100)	51.2 (15.6–75.4)	86.3 (49.6–100)	71.3 (41.0–90.0)

Table 7

Configuration 2: Median (range) of the relative particle concentration [%] for particles $\geq 0.5 \mu m$ ($N = 15$). Measurement positions are shown in Fig. 7. The medians (range) of the four positions together are given in bold italic ($N = 60$).

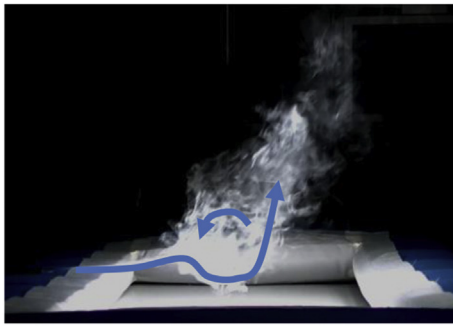
Position	Blanket Series 1	Blanket Series 2	Table Series 1
C_{corner}	22.1 (0.0–52.3)	26.2 (0.0–81.5)	0.2 (0.1–0.4)
C_{c1}	30.5 (19.6–52.3)	27.5 (19.9–40.5)	0.2 (0.1–0.3)
C_{c2}	22.8 (16.2–31.2)	30.5 (18.8–81.5)	0.3 (0.2–0.4)
C_{c3}	22.5 (11.9–51.7)	34.2 (18.5–60.3)	0.3 (0.2–0.3)
C_{c4}	0.0 (0.0–0.0)	0.0 (0.0–0.0)	0.2 (0.1–0.3)
C_{middle}	1.7 (0.5–4.5)	6.1 (0.8–28.5)	0.0 (0.0–0.0)
C_{m1}	1.2 (0.5–2.6)	3.6 (2.7–8.2)	0.0 (0.0–0.0)
C_{m2}	1.5 (1.1–3.0)	5.2 (0.8–9.2)	0.0 (0.0–0.0)
C_{m3}	1.8 (1.1–3.2)	9.5 (3.1–28.5)	0.0 (0.0–0.0)
C_{m4}	2.1 (1.4–4.5)	8.5 (5.5–14.6)	0.0 (0.0–0.0)
$C_{surgeon}$	1.1 (0.3–5.0)	2.0 (0.5–11.4)	1.8 (0.3–4.6)
C_{s1}	1.0 (0.3–3.8)	2.4 (1.4–5.2)	2.0 (0.6–3.5)
C_{s2}	0.8 (0.6–1.7)	1.5 (0.5–2.5)	0.7 (0.3–2.2)
C_{s3}	1.5 (0.7–3.4)	4.6 (1.4–11.4)	2.2 (1.2–4.6)
C_{s4}	1.3 (0.7–5.0)	1.1 (0.7–2.2)	1.9 (1.0–2.7)

performance of all prototypes investigated. Assessment at the surgeon's positions showed significant lower relative particle

concentrations ($p = 0.00$) for Configuration 2 compared to Configuration 1.

3.3. Overall discussion

Based on the results from measurements and simulations the proof-of-principle for the local ventilation system is shown. The outcomes from the full-scale analysis of the prototypes indicate that, based on the assessment procedure prescribed, the solution cannot yet compete on local ventilation efficiency with standard UDF systems as applied currently to arrive at a class 1 OT with performance level 1 [14,50]. This would require a maximum relative particle concentration of 0.1% in the middle of the clean area. It nevertheless can support standard UDF systems near the wound level to reduce disturbance from outside the operating area and, with that, increase robustness in particle-rich situations either inside or outside the UDF supply area. In addition, the local ventilation devices may also already be applicable outside the OT, so operations can be performed more safely in that case (e.g., surgery in temporary OTs during emergency situations or located in developing countries and operations in treatment rooms). For comparison, assuming the HEPA-filtered clean air flow rate as applied for the results shown in Fig. 8, a perfectly mixed situation



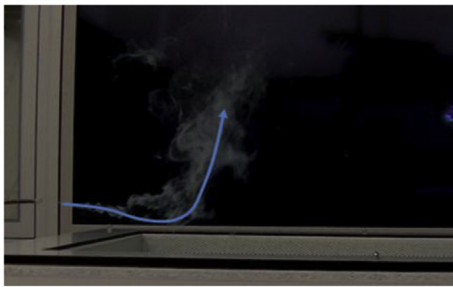
a. Configuration 1 (long side; blanket)



b. Configuration 1 (short side; blanket)



c. Configuration 2 (blanket)



d. Configuration 1 (instrument table)



e. Configuration 2 (instrument table)



f. Configuration 2 (instrument table)

Fig. 11. Smoke tests for the long and short side for the Configuration 1 blanket (a., b.) and the short side for Configuration 2 (c.); and for instrument table Configuration 1 (d.) and Configuration 2 (e., f.). Blue arrows represent the main flow path(s) for the smoke. (For interpretation of the references to colour in this figure legend, the reader is referred to the web version of this article).

would arrive at relative particle concentrations of 94% and 86% for Configuration 1 and Configuration 2 respectively.

The designed and investigated configurations assume a general type of (non-septic) operations. However, the principle may be adapted to serve specific operations and patient positions. In each case care should be given to the local flow conditions. The described assessment procedure may support that analysis. As part of the potential adaptations to the design, size of the open area is also a parameter. From the results (e.g. Fig. 8), the device functions improves for smaller wound areas. In septic operations the distribution of particles may be enhanced with the device developed. This certainly may be assumed for Configuration 1. Though the effect has not been researched, application would not be advised in that case. In general, considerations towards the actual application of the device have not been of concern in this research. Emphasis has been on the proof-of-principle with respect to the ventilation effectiveness, focusing on content validity only. We would certainly recommend to include these considerations in the further evaluation of the configurations to work towards the construct validity. This would also include the assessment method chosen in that case.

The analysis method has a number of limitations. The assessment procedure for the simplified set-up assumes disturbance from the operating personnel and with that may provide a more realistic and conservative assessment of ventilation systems for OT application. The CFD simulations showed that Configuration 2 was more sensitive to the turbulence intensity of the filtered air supply and also to higher supply temperatures. Further analysis should reveal

whether the assumed boundary conditions for clean and contaminated air are too conservative or not. Also an investigation into temporal disturbances, as more representative for the application, may value the credibility of the current approach further.

A similar remark is in place for the full-scale measurements. In the full scale situation it is expected that disturbances in the OT will affect the performance of the local systems less as its functioning depends less on the conditions in the room. The current prescribed assessment procedure only addresses an in rest situation. The wound area, as assumed in the assessment, is relatively large and further performance improvement can be expected with reduction of the wound area that is to be kept clean. The current results nevertheless imply that the local system needs to be combined with an additional room ventilation system to obtain a sufficient performance in case of ultraclean surgery.

Furthermore, the full-scale analysis focused on the wound area and instrument table surface. Exposure to contamination is also possible in the intermediate stage between instrument table and wound area. However, the exposure time for this stage normally would be in the order of seconds. Nevertheless, this would open up the question on further research to time integral exposure of, e.g., instruments to airborne contaminants as an additional (key) performance indicator for these type of systems. The additional room ventilation system may focus on improving the air quality between the blanket and the instrument table (the surgeon's position). Thermal comfort improvement can become part of the focus as well. As reduced flow rates are possible, energy savings can provide

an additional incentive for the further development of the local and room ventilation systems.

The full-scale measurements were significantly hindered by the quality of the prototypes that could be developed, specifically for the blanket design. Though they have been optimized as much as possible before carrying out the full-scale measurements, clear improvements are possible for this design. Besides the flaws in the blankets, the significant differences as found between the two full-scale measurement series for each configuration are further explained by a non-uniform contaminant distribution in the periphery. The contamination mixing in the periphery was constrained as the local ventilation devices required only 6–15% of the air supply rate compared to a standard vertical UDF system (order of 10,000 m³/h). The air in the periphery was not additionally mixed to avoid disturbances in the prescribed measurement set-up. A consistent, uniform distribution of the particles over the room during the measurement period therefore could not be guaranteed.

A more fundamental discussion relates to the assessment procedure in which small particles (0.5–0.7 µm, scalar) are assumed representative for CFUs present in an OT. CFUs can also be much larger. In the analysis and based on earlier research, the flow trajectory of particles up to approximately 10 µm was shown to be represented relatively well by smaller particles in case of clean room air flow characteristics. This is not the case for larger particles (>10 µm) where the effect of external forces may result in significant differences between particle trajectory and air flow streamline. Current guidelines for the assessment of OT ventilation systems do not consider this issue as particle sizes are allowed from 0.5 µm onward. If larger particles would be included in the assessment then this would require a more detailed description of the particle source location and its initial conditions. It is assumed that sources more close to the wound area become of interest then. Most probably an extension of the number of cases then would need to be investigated. In a CFD-simulation setting this may be possible, but validation of the outcomes with experimental data will remain tedious [4,5,51–53].

4. Conclusion

Based on the results obtained, the design solutions proposed are able to provide a cleaner environment near the wound area and instruments' table, when compared to a mixing situation, for contaminant sources from outside the wound area.

The instrument table of Configuration 2 met the guidelines for class 1 Operating Theatres (OT) and could be applied there. For example, as an addition to a vertical UDF system, by placing the ventilating instrument table outside the clean area, the OT clean space can be enlarged. The results of the prototype blankets for both configurations and prototype instrument table for Configuration 1 did not satisfy the guidelines. Further improvements appear possible with improvement of the prototypes. The results obtained from the simplified representation indicate such potential. Besides, the local ventilation devices may certainly be used as a supplement for mixing ventilated OTs to enhance the air quality at the wound level and around the instruments. As a stand-alone device it may support improved air quality conditions for treatments outside standard OT-environments.

These conclusions are based on current standard assessment procedures for general OT ventilation systems. It does not consider the flow path of larger particles (CFUs; size > 10 µm). This asks for improved assessment procedures to investigate the performance to these type of particles as well.

Acknowledgment

The results presented in this article are based on the research conducted by Ivo de Visser and Jelle Loogman for their Master thesis at Eindhoven University of Technology. The mock-up OT in which the full-scale experiments have been performed, the laboratory test setup and prototypes of the instrument tables have been made available for this research by Interflow (BAM Bouw en Techniek bv). They also provided part of the measurement equipment. Royal HaskoningDHV provided materials for developing the prototypes. The authors would like to express their gratitude to Nard van der Sanden, MSc and Remco Noor, MSc from Royal HaskoningDHV and Erik Burgmeijer, MSc and Peter van Wieren from Interflow (BAM Bouw en Techniek bv) for their support and the fruitful discussions related to the work.

References

- [1] PREZIES, Referentiecijfers Module Postoperatieve Wondinfecties 2002–2011, Preventie van Ziekenhuisinfecties door Surveillance (PREZIES), 2012. Available at: http://www.rivm.nl/Onderwerpen/P/PREZIES/Incidentieonderzoek_POWI/Referentiecijfers_POWI (accessed on 18 92015).
- [2] B. Knobben, J.R. van Horn, H.C. van der Mei, H.J. Busscher, Evaluation of measures to decrease intra-operative bacterial contamination in orthopaedic implant surgery, *J. Hosp. Infect.* 62 (2006) 174–180. <http://dx.doi.org/10.1016/j.jhin.2005.08.007>.
- [3] O.M. Lidwell, E.J. Lowbury, W. Whyte, R. Blowers, S.J. Stanley, D. Lowe, Effect of ultraclean air in operating rooms on deep sepsis in the joint after total hip or knee replacement: a randomized study, *Br. Med. J.* 285 (1982) 10–14. <http://dx.doi.org/10.1136/bmj.285.6334.10>.
- [4] S. Sadrizadeh, S. Holmberg, A numerical assessment on different laminar airflow ventilation systems under different clothing systems in an operating room, *J. Infect. Public Health* 7 (6) (2014) 508–516.
- [5] S. Sadrizadeh, S. Holmberg, A. Tammelin, A comparison of vertical and horizontal laminar ventilation systems in an operating room: A numerical study, *Build. Environ.* 82 (2014) 517–525. <http://dx.doi.org/10.1016/j.buildenv.2014.09.013>.
- [6] W.A.C. Zoon, M.G.L.C. Loomans, J.L.M. Hensen, Testing the effectiveness of operating room ventilation with regard to removal of airborne bacteria, *Build. Environ.* 46 (12) (2011) 2570–2577. <http://dx.doi.org/10.1016/j.buildenv.2011.06.015>.
- [7] M. Loomans, Houdt W. van, A.D. Lemaire, J.L.M. Hensen, Performance assessment of an operating theatre design using CFD simulation and tracer gas measurements, *Indoor Built Environ.* 17 (4) (2008) 299–312. <http://dx.doi.org/10.1177/1420326X08094948>.
- [8] T.T. Chow, X.Y. Yang, Ventilation performance in the operating theatre against airborne infection: numerical study on an ultra-clean system, *J. Hosp. Infect.* 59 (2) (2005) 138–147. <http://dx.doi.org/10.1016/j.jhin.2004.09.006>.
- [9] W. Whyte, O.M. Lidwell, E.J.L. Lowbury, R. Blowers, Suggested bacteriological standards for air in ultraclean operating rooms, *J. Hosp. Infect.* 4 (1983) 133–139. [http://dx.doi.org/10.1016/0195-6701\(83\)90042-7](http://dx.doi.org/10.1016/0195-6701(83)90042-7).
- [10] D.F. De Korne, J.D. Van Wijngaarden, R.J. Van Rooij, L.S. Wauben, U.F. Hiddema, N.S. Klazinga, Safety by design: effects of operating room floor marking on the position of surgical devices to promote clean air flow compliance and minimize infection risks, *Br. Med. J.* 21 (2012). <http://dx.doi.org/10.1136/bmjqs-2011-000138>.
- [11] W.A.C. Zoon, Heijden MGM van der, M.G.L.C. Loomans, J.L.M. Hensen, On the applicability of the laminar flow index when selecting surgical lighting, *Build. Environ.* 45 (2010) 1976–1983. <http://dx.doi.org/10.1016/j.buildenv.2010.02.011>.
- [12] H. Brohus, K.D. Balling, D. Jeppesen, Influence of movements on contaminant transport in an operating room, *Indoor Air* 16 (2006) 356–372. <http://dx.doi.org/10.1111/j.1600-0668.2006.00454.x>.
- [13] R. Van Gaever, V.A. Jacobs, M. Diltoer, L. Peeters, S. Vanlanduit, Thermal comfort of the surgical staff in the operating room, *Build. Environ.* 81 (2014) 37–41. <http://dx.doi.org/10.1016/j.buildenv.2014.05.036>.
- [14] WIP, *Luchtbehandeling in operatiekamer en opdekruimte in operatieafdeling klasse 1*, Werkgroep Infectie Preventie (WIP), Leiden, The Netherlands, 2014, p. 69.
- [15] S.M. Levenson, P.C. Trexler, D van der Waaij, Nosocomial infection: prevention by special cleanair, ultraviolet light, and barrier (isolator) techniques, *Curr. Problems Surg.* 23 (7) (1986) 458–558. [http://dx.doi.org/10.1016/0011-3840\(86\)90033-X](http://dx.doi.org/10.1016/0011-3840(86)90033-X).
- [16] P. Ham, *Handboek Ziekenhuis Ventilatie*, TNO Preventie en gezondheid, Leiden, The Netherlands, 2002.
- [17] J.R. Babb, P. Lynam, G.A.J. Ayliffe, Risk of airborne transmission in an operating theatre containing four ultraclean air units, *J. Hosp. Infect.* 31 (1995) 159–168. [http://dx.doi.org/10.1016/0195-6701\(95\)90062-4](http://dx.doi.org/10.1016/0195-6701(95)90062-4).
- [18] W. Whyte, B.H. Shaw, R. Barnes, A bacteriological evaluation of laminar-flow

- systems for orthopaedic surgery, *J. Hyg.* 71 (1973) 559–564. <http://dx.doi.org/10.1017/S0022172400046544>.
- [19] Surgicube (2013) Available at: <http://www.nios.com/mydownloads/Surgicube%20ENG.pdf> (accessed on: 22-01-2016).
- [20] MediShield (2012) Available at: <http://www.medishieldelft.com/projects/shaftshield/> (accessed on: 22-01-2016).
- [21] D. van der Waaij, N. Wieggersma, J. Dankert, Bacteriological evaluation of a mobile laminar cross-flow unit for surgery, under laboratory circumstances, *J. Hyg.* 76 (1976) 1–10. <http://dx.doi.org/10.1017/S0022172400054887>.
- [22] W. Whyte, A. Hambræus, G. Laurell, J. Hoborn, The relative importance of the routes and sources of wound contamination during general surgery. II. Airborne, *J. Hosp. Infect.* 22 (1992) 41–54.
- [23] B. Friberg, M. Lindgren, C. Karlsson, A. Bergström, S. Friberg, Mobile zoned/exponential LAF screen: a new concept in ultra-clean air technology for additional operating room ventilation, *J. Hosp. Infect.* 50 (2002) 286–292. <http://dx.doi.org/10.1053/jhin.2001.1164>.
- [24] S. Friberg, B. Ardnor, R. Lundholm, B. Friberg, The addition of a mobile ultra-clean exponential laminar airflow screen to conventional operating room ventilation reduces bacterial contamination to operating box levels, *J. Hosp. Infect.* 55 (2003) 92–97. [http://dx.doi.org/10.1016/S0195-6701\(03\)00143-9](http://dx.doi.org/10.1016/S0195-6701(03)00143-9).
- [25] M. Thore, L.G. Burman, Further bacteriological evaluation of the TOUL mobile system delivering ultra-clean air over surgical patients and instruments, *J. Hosp. Infect.* 63 (2006) 185–192. <http://dx.doi.org/10.1016/j.jhin.2005.12.011>.
- [26] C. Pasquarella, G.E. Sansebastiano, S. Ferretti, E. Sacconi, M. Fanti, U. Moscato, G. Giannetti, S. Fornia, P. Cortellini, P. Vitali, C. Signorelli, A mobile laminar airflow unit to reduce air bacterial contamination at surgical area in a conventionally ventilated operating theatre, *J. Hosp. Infect.* 66 (2007) 313–319. <http://dx.doi.org/10.1016/j.jhin.2007.05.022>.
- [27] D. Sossai, G. Dagnino, F. Sanguineti Fand Franchin, Mobile laminar air flow screen for additional operating room ventilation: reduction of intraoperative bacterial contamination during total knee arthroplasty, *J. Orthopaedics Traumatology* 12 (2011) 207–211. <http://dx.doi.org/10.1007/s10195-011-0168-5>.
- [28] G.W. Stocks, D.P. O'Connor, S.D. Self, G.A. Marcek, B.L. Thompson, Directed Air Flow to Reduce Airborne Particulate and Bacterial Contamination in the Surgical Field During Total Hip Arthroplasty, *J. Arthroplasty* 26 (5) (2011) 771–776. <http://dx.doi.org/10.1016/j.arth.2010.07.001>.
- [29] J.M. Frey, M. Janson, M. Svanfeldt, P.K. Svenarud, J.A. van der Linden, Local insufflations of warm humidified CO₂ increases open wound and core temperature during open colon surgery: a randomized clinical trial, *Int. Anesth. Res. Soc.* 115 (2012) 5.
- [30] H. Klems, Z. Nouri, S. Kecskés, H. Esdorn, Das Reinfeldverfahren zur lokalen Keimreduzierung in Operationsräumen, *Unfallchirurgie* 7 (4) (1981) 215–220.
- [31] M. Persson, J. van der Linden, Wound ventilation with carbon dioxide: a simple method to prevent direct airborne contamination during cardiac surgery? *J. Hosp. Infect.* 56 (2004) 131–136. <http://dx.doi.org/10.1016/j.jhin.2003.10.013>.
- [32] A. Melikov, Personalized ventilation, *Indoor Air* 14 (7) (2004) 157–167. <http://dx.doi.org/10.1111/j.1600-0668.2004.00284.x>.
- [33] A. Melikov, T. Ivanova, G. Stefanova, Seat headrest-incorporated personalized ventilation: thermal comfort and inhaled air quality, *Build. Environ.* 47 (2012) 100–108. <http://dx.doi.org/10.1016/j.buildenv.2011.07.013>.
- [34] P.V. Nielsen, Control of airborne infectious diseases in ventilated spaces, *J. R. Soc. Interface* 6 (2009) S747–S755. <http://dx.doi.org/10.1098/rsif.2009.0228.focus>.
- [35] J.G.H. Loogman, I.M. de Visser, Alternative Ventilation Systems for the Operating Theatre – a Literature Study. Master Report, Department Built Environment. Eindhoven University of Technology, Eindhoven, 2014, p. 113.
- [36] 3M (2015) Website: [http://solutions.3m.com/wps/portal/3M/en_US/IPD-NA/3M-Infection-Prevention/catalog/\(product: 3M™ Bair Hugger™ Surgical Access Blanket, Model 570\).](http://solutions.3m.com/wps/portal/3M/en_US/IPD-NA/3M-Infection-Prevention/catalog/(product: 3M™ Bair Hugger™ Surgical Access Blanket, Model 570).) (accessed on: 17-08-2015).
- [37] K. Woodhead, E.W. Taylor, G. Bannister, T. Chesworth, P. Hoffman, H. Humphreys, Behaviours and rituals in the operating theatre, *J. Hosp. Infect.* 51 (2002) 241–255. <http://dx.doi.org/10.1053/jhin.2002.1220>.
- [38] D. Hansen, C. Krabs, D. Benner, A. Brauksiepe, W. Popp, Laminar air flow provides high air quality in the operating field even during real operating conditions, but personal protection seems to be necessary in operations with tissue combustion, *Environ. Health* 208 (2005) 455–460. <http://dx.doi.org/10.1016/j.ijheh.2005.08.008>.
- [39] S. Scaltriti, S. Cencetti, s. Rovesti, I. Marchesi, A. Bargellini, P. Borella, Risk factors for particulate and microbial contamination of air in operating theatres, *J. Hosp. Infect.* 66 (2007) 320–326. <http://dx.doi.org/10.1016/j.jhin.2007.05.019>.
- [40] W.C. Noble, O.M. Lidwell, D. Kingston, The size distribution of airborne particles carrying micro-organisms, *J. Hyg.* 61 (1963) 385–391. <http://dx.doi.org/10.1017/S0022172400020994>.
- [41] J. Gralton, E. Tovey, M. McLaws, W.D. Rawlinson, The role of particle size in aerosolized pathogen transmission: a review, *J. Infect.* 62 (2011) 1–13. <http://dx.doi.org/10.1016/j.jinf.2010.11.010>.
- [42] J.W. Tang, Y. Li, I. Eames, P.K.S. Chan, G.L. Ridgway, Factors involved in the aerosol transmission of infection and control of ventilation in healthcare premises, *J. Hosp. Infect.* 64 (2006) 100–114. <http://dx.doi.org/10.1016/j.jhin.2006.05.022>.
- [43] I.B.M. Corp, IBM SPSS Statistics for Windows, Version 22.0 (Released 2013), IBM Corp, Armonk, NY, 2013.
- [44] A.N.S.Y.S. Fluent, ANSYS Fluent User's Guide. Release 14.0, 2011 (Lebanon, USA).
- [45] T.T. Chow, X.Y. Yang, Performance of ventilation system in a non-standard operating room, *Build. Environ.* 38 (12) (2003) 1401–1411. [http://dx.doi.org/10.1016/S0360-1323\(03\)00155-0](http://dx.doi.org/10.1016/S0360-1323(03)00155-0).
- [46] A.K. Melikov, Z. Popiolek, M.C.G. Silva, I. Care, T. Sefker, Accuracy limitation for low-velocity measurements and draft assessment in rooms, *HVAC&R Res.* 13 (6) (2007) 971–986. <http://dx.doi.org/10.1080/10789669.2007.10391465>.
- [47] M.G.L.C. Loomans, A.W.M. Van Schijndel, Simulation and measurement of the stationary and transient characteristics of the hot sphere anemometer, *Build. Environ.* 37 (2002) 153–163. [http://dx.doi.org/10.1016/S0360-1323\(01\)00019-1](http://dx.doi.org/10.1016/S0360-1323(01)00019-1).
- [48] T. Van Hooff, B. Blocken, Coupled urban wind flow and indoor natural ventilation modelling on a high-resolution grid: a case study for the Amsterdam ArenA stadium, *Environ. Model. Softw.* 25 (2010) 51–65. <http://dx.doi.org/10.1016/j.envsoft.2009.07.008>.
- [49] T. Van Hooff, B. Blocken, G.J.F. Van Heijst, On the suitability of steady RANS CFD for forced mixing ventilation at transitional slot Reynolds numbers, *Indoor Air* 23 (2013) 236–249. <http://dx.doi.org/10.1111/ina.12010>.
- [50] VCCN RL7, Methode voor testen en classificeren van operatiekamers en opdekruimtes in rust. Vereniging Contamination Control Nederland (VCCN). Leusden, The Netherlands, in: Dutch: Method for Testing and Classification of Operating Theatres and Preparation Rooms at Rest, 2014.
- [51] S. Sadrizadeh, A. Tammelin, P. Ekolind, S. Holmberg, Influence of staff number and internal constellation on surgical site infection in an operating room, *Particuology* 13 (2014) 42–51. <http://dx.doi.org/10.1016/j.partic.2013.10.006>.
- [52] M.-F. King, C.J. Noakes, P.A. Sleigh, M.A. Camargo-Valero, Bioaerosol deposition in single and two-bed hospital rooms: A numerical and experimental study, *Build. Environ.* 59 (2013) 436–447. <http://dx.doi.org/10.1016/j.buildenv.2012.09.011>.
- [53] S. Liu, A. Novoselac, Lagrangian particle modeling in the indoor environment: A comparison of RANS and LES turbulence methods (RP-1512), *HVAC&R Res.* 20 (2014) 480–495. <http://dx.doi.org/10.1080/10789669.2014.884380>.